Primeval Aptian marine incursions in the interior of Northeastern Brazil following the Gondwana breakup

Gerson Fauth (gersonf@unisinos.br)
Instituto Tecnológico de Paleoceanografia e Mudanças Climáticas (itt Oceaneon), Unisinos University, Avenida Unisinos, 950 - Cristo Rei, São Leopoldo, RS 93022-750, Brazil

Henrique Parisi Kern
Instituto Tecnológico de Paleoceanografia e Mudanças Climáticas (itt Oceaneon), Unisinos University, Avenida Unisinos, 950 - Cristo Rei, São Leopoldo, RS 93022-750, Brazil

Jorge Villegas-Martín
Instituto Tecnológico de Paleoceanografia e Mudanças Climáticas (itt Oceaneon), Unisinos University, Avenida Unisinos, 950 - Cristo Rei, São Leopoldo, RS 93022-750, Brazil

Marcelo Augusto de Lira Mota
Instituto Tecnológico de Paleoceanografia e Mudanças Climáticas (itt Oceaneon), Unisinos University, Avenida Unisinos, 950 - Cristo Rei, São Leopoldo, RS 93022-750, Brazil

Marcos Antonio Batista dos Santos Filho
Instituto Tecnológico de Paleoceanografia e Mudanças Climáticas (itt Oceaneon), Unisinos University, Avenida Unisinos, 950 - Cristo Rei, São Leopoldo, RS 93022-750, Brazil

Amanda Santa Catharina
São Paulo State University – Unesp, Department of Geology, Rio Claro, SP, Brazil

Lilian Maia Leandro
Instituto Tecnológico de Paleoceanografia e Mudanças Climáticas (itt Oceaneon), Unisinos University, Avenida Unisinos, 950 - Cristo Rei, São Leopoldo, RS 93022-750, Brazil

Fernanda Luft-Souza
Instituto Tecnológico de Paleoceanografia e Mudanças Climáticas (itt Oceaneon), Unisinos University, Avenida Unisinos, 950 - Cristo Rei, São Leopoldo, RS 93022-750, Brazil

Oscar Strohschoen Jr.
Instituto Tecnológico de Paleoceanografia e Mudanças Climáticas (itt Oceaneon), Unisinos University, Avenida Unisinos, 950 - Cristo Rei, São Leopoldo, RS 93022-750, Brazil

Andressa Nauter-Alves
Instituto Tecnológico de Paleoceanografia e Mudanças Climáticas (itt Oceaneon), Unisinos University, Avenida Unisinos, 950 - Cristo Rei, São Leopoldo, RS 93022-750, Brazil

Edna de Jesus Francisco Tungo

Instituto Tecnológico de Paleoceanografia e Mudanças Climáticas (itt Oceaneon), Unisinos University, Avenida Unisinos, 950 - Cristo Rei, São Leopoldo, RS 93022-750, Brazil

Mauro Daniel Rodrigues Bruno

Instituto Tecnológico de Paleoceanografia e Mudanças Climáticas (itt Oceaneon), Unisinos University, Avenida Unisinos, 950 - Cristo Rei, São Leopoldo, RS 93022-750, Brazil

Daiane Ceolin

Instituto Tecnológico de Paleoceanografia e Mudanças Climáticas (itt Oceaneon), Unisinos University, Avenida Unisinos, 950 - Cristo Rei, São Leopoldo, RS 93022-750, Brazil

Simone Baecker-Fauth

Instituto Tecnológico de Paleoceanografia e Mudanças Climáticas (itt Oceaneon), Unisinos University, Avenida Unisinos, 950 - Cristo Rei, São Leopoldo, RS 93022-750, Brazil

Marlone Heliara Hüning Bom

Instituto Tecnológico de Paleoceanografia e Mudanças Climáticas (itt Oceaneon), Unisinos University, Avenida Unisinos, 950 - Cristo Rei, São Leopoldo, RS 93022-750, Brazil

Francisco Henrique de Oliveira Lima

Petrobras, Research Center (CENPES), Av. Horácio Macedo, 950, Cidade Universitária, Ilha do Fundão, Rio de Janeiro, RJ, 21941-915, Brazil

Mario Luis Assine

São Paulo State University – Unesp, Department of Geology, Rio Claro, SP, Brazil

---

Article

Keywords: Araripe Basin, Barbalha Formation, Early Cretaceous, Marine microfossils, Planktonic Foraminifera

Posted Date: May 31st, 2022

DOI: https://doi.org/10.21203/rs.3.rs-1674479/v1

Additional Declarations: No competing interests reported.

Version of Record: A version of this preprint was published at Scientific Reports on April 25th, 2023. See the published version at https://doi.org/10.1038/s41598-023-32967-w.

Abstract

This study reports a set of primeval marine incursions identified in the two drill cores (1PS-06-CE and 1PS-10-CE) recovering the Barbalha Formation, Araripe Basin, Brazil. Based on multi-proxy approach involving stratigraphy, microbiofacies, ichnofossils, and microfossils found in the Barbalha Formation, three short-lived marine incursions were identified, designated Araripe Marine Incursions (AMI). The AMI-1 and AMI-2, which occur within the shaly Batateira Beds (lower part of the Barbalha Formation), were identified through the occurrence of benthic foraminifera, calcareous nannofossils, dinocysts, and a mass mortality event of non-marine ostracods. The AMI-3 is recorded in the upper part of the Barbalha Formation and its identification was based on occurrence of ichnofossils and planktic foraminifers. The presence of planktic foraminifera genus *Leupoldina* suggests, for the first time in the basin, an early Aptian/early late Aptian age for the deposits and allows correlation of this unit with global foraminifera biozonation. Our findings have implications for the breakup of the Gondwana Supercontinent, as these incursions represent the earliest marine-derived flooding in the inland basins of Northeastern Brazil.

Introduction

The Aptian (126.3 to 113.1 Ma[1]) is an important stage of the Early Cretaceous, characterized by significant paleogeographic and paleoceanographic events around the world. Oceanic gateways gradually opened during this stage, and rising sea levels allowed the dispersion of marine biota (e.g.,[2–5]). During the Early Cretaceous, the Gondwana Supercontinent broke up into the South American and African continents, leading to the establishment of the South Atlantic Ocean (e.g.,[5–8]).

The initial evolution of the South Atlantic Ocean has been widely debated in terms of relative motion and timing. Reversal-related magnetic anomalies indicate the onset of the opening around Anomaly M13 (134 Ma[9,10]) in the Austral Atlantic Ocean, but the Cretaceous Magnetic Quiet Zone (CMQZ – 121 Ma, Anomaly M0, to 83.6 Ma (Anomaly C34[11,12]) complicates age determination for its subsequent spread northwards, between the Barremian and Aptian interval.

Identification of the source and pathways taken by the first marine flooding episodes from the South Atlantic Ocean in the Brazilian intracratonic sedimentary basins is further complicated by conflicting results based on paleontological and sedimentary proxies (e.g.,[13–16]). Paleontological data supports a clear connection with Tethyan sea waters (e.g.,[13,17–21]), while a combination of stratigraphy and geometry of the deposits establishes a transgression path from south to north and further inland[14,22,23].

The geological record of Northeastern Brazilian marginal and interior basins is fundamental for providing temporal and geographical constraints for the first marine incursions in the region, including their provenance and relationship with the relative motions between the incipient African and South American plates. A combination of paleontological, sedimentological, stratigraphic, and geochemical approaches is essential to obtain a clearer image of these ingressions, and therefore the relationship between waters of the Tethys and proto-South Atlantic, as well as developing a more accurate paleogeographical model for

this time interval. The recognition of marine incursions within these basins gives essential information is essential to decipher pathways and ways of this major geological event.

In this study, we provide a multi-proxy analysis of two boreholes, 1PS-06-CE and 1PS-10-CE, from the eastern portion of the Araripe Basin, Northeast Brazil, a large interior basin whose origin is related to the breakup of the Gondwana[23–26], and in which late Aptian–early Albian marine incursions have been previously identified (e.g.,[13,14,27–32]). These yielded new ichnological, micropaleontological, and microbiofaciological records of the Barbalha Formation which is the lowermost stratigraphic unit of the basin´s post-rift sequence, allowing for the identification of the primeval marine incursions in Northeastern Brazil.

- Geological setting

The Araripe Basin is a large inland basin in northeastern Brazil associated with the opening of the South Atlantic Ocean[22]. Its development, along several other rift basins in Brazil, was triggered by the breakup of the Gondwana Supercontinent during the Cretaceous[23–26, 33], and its deposits lay atop Precambrian terrains (Piancó-Alto Brígida and Granjeiro), in the transversal domain of the Borborema Province, to the south of the Patos Shear Zone.

The Santana Group (*sensu* Neumann and Assine[34]) is the stratigraphic record of the local Alagoas Stage (Aptian/lower Albian), equivalent to the post-rift I megasequence[23]. The precise age of the deposits of this group is the subject of considerable debate (e.g.,[13,27,28,30,31,35–37]). This unit has been typically assigned to the Aptian, though several studies place the upper part of this unit (Romualdo Formation) in the Aptian–Albian interval (e.g.,[27,32,35]).

The sedimentary succession of the Santana Group is represented by the Barbalha, Crato, Ipubi, and Romualdo formations (Fig. 1), from base to top, and comprise mixed carbonate-siliciclastic sediments, deposited during the post-rift stage[14,23]. The Barbalha Formation, focus of this study, is divided into two parts. The lower one is essentially siliciclastic, passing from a fluvial to a lacustrine continental environment in a transgressive pattern that culminates in the Batateira Beds, a laterally extensive layer of mudstones and marls that are an important stratigraphic mark for the basin[14]. The fossils preservation pattern has been used to interpret continental environments, with some dysoxic/anoxic intervals for this unit[23,24,38–40]. The upper part of the Barbalha Formation is composed of a siliciclastic succession of sandstones and mudstones with a fining upward pattern that ends with the deposition of laminated limestones of the Crato Formation. This reflects a change from fluvial settings to hypersaline lacustrine environments (e.g.,[41–43]).

Widespread marine ingressions have been previously recorded in the Araripe Basin for the Romualdo Formation, during the late Aptian[14,44–46]. Its deposits of black shales with fossil-bearing carbonate concretions (e.g.,[28,47,48]) are famous for their well-preserved fossils, and includes continental (palynomorphs and ostracods[27]) as well as marine groups, including dinoflagellates[30,49,50], benthic and

planktonic foraminifera[31,32], marine ostracods[32], and calcareous nannofossils[32]. The distribution of these marine organisms, many related to the Tethyan Realm, suggests short marine incursions from the Central Atlantic Ocean (e.g.,[13,16,32,51]). These marine incursions could have occurred due to sufficient tectonic subsidence rates accompanied by rising sea level episodes[52,53], possibly entering repeatedly at different times during the Early Cretaceous.

Results

Sedimentology and ichnology

We have recognized 16 sedimentary facies in the Barbalha Formation, identified and described in Table 1. The lower part comprises sandstones and rare muddy deposits which are overlain by muddy, locally carbonate deposits (Batateira Beds), with low ichnodiversity and low rates on the bioturbation scale. The upper part is characterized by sandstone cosets (locally bioturbated), occasionally intercalated with fine-grained deposits (Fig. 2), which are overlaid by an interval dominated by muddy deposits interbedded with sandstone beds.

Table 1
Sedimentary lithofacies identified in the Barbalha Formation

Lithoacies code	Description	* Bioturbation / Bioturbation scale (BS)	Formation
Fs	Dark gray clayey shale with moderate fissility. Sparse occurrence of bivalve shell impression (~ 2 mm).	Ch / BS-1; Th / BS 2	Barbalha (lower)
F1	Medium gray to grey-green silty shale, massive to laminated, low fissility, micaceous, occasionally interbedded with lamina of very fine-grained sandstone forming centimeter heterolithic levels. Fluidized levels occur. Locally, with abundant plant debris.	Pl / BS 1; Th/ BS 1; Th-Pl / BS 1	Barbalha (lower)
F2	Medium gray to cream-grey siltstone, with yellowish and reddish spots, micaceous and laminated. Rarely interbedded with discrete lamina of very fin-grained sandstone.	Ch / BS-1; Pl / BS 1	Barbalha (lower and upper)
F3	Reddish-gray to light reddish-brown siltstone to claystone with greenish-gray spots, micaceous, massive to laminated. Thin levels of silty sandstone and fluidized levels occur. Intervals with blocky texture and slickensides structure also occur (paleosol).	Rhizobioturbation	Barbalha (upper)
M	Light gray marl, massive to laminated. Moderate to strong effervescence at 10% HCl.	Th / BS 1–2; Ch-Pa / BS 1–2	Barbalha (lower and upper)
Hsr	Heterolith composed of centimetric lamina of very fine-grained sandstone interbedded with centimetric lamina of dark gray siltstone. The sandstone lamina present unidirectional cross-lamination, occasionally with claystone flaser bedding. Levels with moderate bioturbation and fluidized levels occur.	Pa-Pl-Th / BS 1–2; Pa-Pl / BS 1–2; Th / BS 2–3.	Barbalha (lower and upper)
C	Laminite composed of millimetric to centimetric levels of thin beds of fine-grained limestone with parallel and/or crenulate lamination, interlayered with millimetric to centimetric beds of dark shale. Common occurrence of oval-shaped carbonate nodules and spherical carbonate concretions (pisoliths?). Convoluted aspect in 1PS-06-CE borehole. Petrographic analyzes reveal that the limestone is composed of ostracod wackstone and packstone, and microbially induced sedimentary structures (MISS).	Pa-Ch / BS 1–2	Barbalha (lower)

* Ichnofossils: Ch = *Chondrites* isp.; Th = *Thalassinoides* isp.; Pl = *Planolites* isp.; Pa = *Palaeophycus* isp.; Di = *Diplocraterion* isp.; Cy = *Cylindrichnus* isp.; He = *Helminthopsis* isp.; Sc = *Scolicia* isp.; Op = *Ophiomorpha* isp.; Sk = *Skolithos* isp.; Te = *Teichichnus* isp.; As = *Asterosoma* isp.; and Lo = *Lockeia* isp.

Lithoacies code	Description	* Bioturbation / Bioturbation scale (BS)	Formation
Sr	Very fine- to fine-grained sandstone, cream-yellow to reddish, composed of sub-rounded to rounded quartz and feldspar grains, and lamellae of mica. Present unidirectional cross-lamination.	Pa-Pl / BS 1–2 / Pa-Pl-?As / BS 1–2 / Th / BS 1	Barbalha (lower and upper)
Srw	Very fine-grained gray sandstone, composed of sub-rounded quartz grains, white mica lamellae and gray claystone intraclasts. Present bidirectional cross lamination with heavy minerals in the lamination planes. Moderate to intense bioturbation (vertical and horizontal pattern).	Sc-Th-Di-Pa-Pl-Ch-Lo / BI 4–5; Op-Th-Pa-Pl-He-Di-?Sk / BI 4–5. Figure 2A-C; F.	Barbalha (upper)
Srd	Very fine- to fine grained- sandstone, gray, composed of sub-rounded quartz grains, opaque minerals, white mica lamellae and gray claystone rip-up clasts. Present unidirectional cross-lamination with drape bedding. Moderate to intense bioturbation (vertical and horizontal pattern).	Th / IB 1; Di-Pa-Pl-Th-Ch-Cy-He / BI 4–5; Di-Pa-Pl-?Sc-He-Th / BI 4; Th-Sc-Pa-Pl-Di-He / IB 4; Sk-Di-Pa-Pl-Cy-Bi / IB 3–4; Th-Pa-Pl / IB 2; Th-Pa-Pl / IB 2; Pa-Pl / IB 1–2; Pa-Pl-Cy / BS 1–2. Figure 2D-E; G.	Barbalha (upper)
Sm1	Very fine-grained sandstone, grey and massive. Bioturbated appearance.	Bioturbated aspect when associated with St4 facies.	Barbalha (upper)
Sm2	Medium- to coarse-grained sandstone, gray-white in color, massive, composed of sub-rounded grains of quartz and feldspar, intensely cemented by CaCO3.	-	Barbalha (upper)
St1	Fine- to very coarse -grained sandstone, brownish-yellow, composed of sub-rounded quartz and feldspar grains, mica lamellae. Present small to medium-scale trough cross-bedding (10–30 cm).	-	Barbalha (lower and upper)
St2	Fine- to medium-grained sandstone, gray, with small- to medium-scale trough cross bedding. Composed of rounded to subrounded grains of quartz, feldspar, opaque minerals and lamellae of mica. Heavy minerals are concentrated in the bedding planes and levels with claystone intraclasts may occur. In the 1PS-06-CE well there are massive levels associated with intense bioturbation (Sm1).	Pa-Pl / BS 1–2; Di-Th-Cy-Pa-Pl-Te-Ch-?Sk / BS 4–5; Te-Th-Pa-Pl-He-Di / IB 4–5. Figure 2H.	Barbalha (upper)

* Ichnofossils: Ch = *Chondrites* isp.; Th = *Thalassinoides* isp.; Pl = *Planolites* isp.; Pa = *Palaeophycus* isp.; Di = *Diplocraterion* isp.; Cy = *Cylindrichnus* isp.; He = *Helminthopsis* isp.; Sc = *Scolicia* isp.; Op = *Ophiomorpha* isp.; Sk = *Skolithos* isp.; Te = *Teichichnus* isp.; As = *Asterosoma* isp.; and Lo = *Lockeia* isp.

Lithoacies code	Description	* Bioturbation / Bioturbation scale (BS)	Formation
Sgt	Pebbly sandstone with medium-grained quartz-feldspathic matrix, light gray, with small-scale trough cross-bedding (10 cm). It presents granules and small pebbles of quartz and altered feldspar (kaolin).	-	Barbalha (upper)
Gt	Small- to medium-size coble conglomerate with fine- to coarse-grained sandstone matrix, composed of angular and sub-rounded quartz and feldspar grains, and mica lamellae, with small-scale trough cross-bedding (10 cm). The pebbles are subrounded to subangular, small to medium size composed of quartz and feldspar, in addition to lithic fragments (granitoids).	-	Barbalha (upper)
* Ichnofossils: Ch = *Chondrites* isp.; Th = *Thalassinoides* isp.; Pl = *Planolites* isp.; Pa = *Palaeophycus* isp.; Di = *Diplocraterion* isp.; Cy = *Cylindrichnus* isp.; He = *Helminthopsis* isp.; Sc = *Scolicia* isp.; Op = *Ophiomorpha* isp.; Sk = *Skolithos* isp.; Te = *Teichichnus* isp.; As = *Asterosoma* isp.; and Lo = *Lockeia* isp.			

Ostracods

Eight species belonging to three genera of non-marine ostracods were identified in borehole 1PS-06-CE, (Fig. 3A-H). Recovered species include *Candonopsis alagoensis*, *Candona*? sp., *Pattersoncypris alta*?, *Pattersoncypris micropapillosa*, *Pattersoncypris salitrensis, Pattersoncypris angulata* (sensu Tomé et al.[29]) *Pattersoncypris* sp. 1, and *Pattersoncypris* sp. 2. Fossil preservation ranged from moderate to good.

Ostracod abundance varies throughout this borehole (1PS-06-CE). Between depths 112.30 and 92.40 m, which encompasses the Batateira Beds, there is a remarkably high abundance of well-preserved and articulated specimens (particularly at depths 99.80 and 99.30 m, with over 1,000 individuals each sample), including many younger ontogenetic stages. Between the depths of 91.45 and 13.60 m, there is a considerable decrease in abundance and diversity of the ostracod fauna.

Comparatively, abundance and diversity are overall low in borehole 1PS-10-CE, and fossil preservation is moderate to poor. The samples with the highest abundance are in the laminites of the Batateira Beds (101.54 m). Six species belonging to six genera of non-marine ostracods were recovered (Fig. 3A-H): *Candonopsis alagoensis*, *Cypridea* sp., *Brasacypris subovatum, Pattersoncypris* sp. 3, *Theriosynoecum silvai*, as well as one Gen. et sp. *indet* ostracod.

Benthic Foraminifera

Abundant associations of agglutinated benthic foraminifera, classified as *Bathysiphon* sp., were found near the base of the Batateira Beds in both boreholes (117.90 m in 1PS-06-CE and 105.90, 103.20, and 102.90 m in 1PS-10-CE) (Fig. 3I-M). Specimens are well-preserved but usually fragmented and characterize monofaunistic occurrences.

Calcareous nannofossils

Calcareous nannofossils were recovered in borehole 1PS-06-CE, but not in 1PS-10-CE. In the fine-grained facies of the Batateira Beds (Fig. 3N-U), we recorded badly to well-preserved ascidian spicules at 112.30 m and five specimens of calcareous dinocyst fragments (*Thoracosphaera* spp.) at 114.70 m.

We also observed 24 specimens of ascidian spicules at 99.30 m, the most abundant calcareous nannofossil assemblage of the borehole. They show diverse morphologies (rounded, spheric, and radial shapes) as well as dissolution/overgrowth preservation effects. Four specimens of *Thoracosphaera* spp. found at 99.30 m have morphologies marked by fragments with large inner element sizes and low preservation.

Microbiofacies

Based on thin microbiofacies sections of borehole 1PS-06-CE, we observed two horizons with marine microfossils (serpulids and foraminifera) in the Barbalha Formation (Fig. 4A-J).

The first horizon consists of interbedded wackestone and packstone beds at the depth 99.30 m, and include abundant ostracods (in situ and reworked), serpulid tubes (Fig. 4G-J), microbial peloids, organic matter, and calcareous concretions. Two distinct ostracod deposits were preserved in the laminites of this interval: a packstone with disarticulated and compressed ostracod valves (Fig. 4H), and a wackestone with articulated, adult- to juvenile-sized ostracod carapaces, associated with serpulid tubes in an organic-rich matrix (Fig. 4J). The serpulid tubes are 50-to 250 μm long, showing good preservation with partial dissolution and local compression. They are most abundant on the organic muddy microbial matrix among ostracod valves (Fig. 4G-J), but are absent in the ostracod packstone.

The second horizon is represented by the reddish-brown mudstone of the F3 facies, locally brecciated, occurring at 39.20 m. Planktonic foraminifera are frequent (Fig. 4A-6D), and include the genera *Leupoldina* and *Globigerinelloides*. Most specimens have undergone some degree of dissolution, and internal molds, partially dissolved tests, and ghosts are frequent. Taxonomic identification is possible at generic level (*Leupoldina* spp.) and even at specific level in some cases (*Globigerinelloides* cf. *barri* and *G.* cf. *ferreolensis*) (Fig. 4A-D).

Organic-walled microfossils

Pollen grains and plant spores are responsible for the majority of palynomorph counts in samples from borehole 1PS-06-CE, followed by freshwater algae (2%: *Botryococcus* spp., and *Pediastrum* spp.), and dinocysts (< 1%: *Oligosphaeridium* spp., *Subtilisphaera* spp. and *Exochosphaeridium* spp.) (Fig. 4K-O). Marked presence of dinocysts (up to 10%) is observed at 111.97–86.39 m. Sporomorphs also represent most palynomorphs at borehole 1PS-10-CE, followed by freshwater algae (3%: *Botryococcus* spp., and *Pediastrum* spp.), and dinocysts (1%: *Subtilisphaera* spp.). This borehole has a marked abundance of salinity-indicative palynomorphs (12%; i.e., *Exochosphaeridium* spp., *Oligosphaeridium* spp., and *Subtilisphaera* spp.) at 105.90–95.76 m.

Discussion

Biostratigraphic framework and age controls

The absence of globally distributed marine microfossils in the Brazilian interior basins prevented their correlation with global chronostratigraphic charts, and has thus so far only been calibrated using local biozones. Here we report for the first time the occurrence of *Leupoldina* spp. in the Barbalha Formation, as per observation in thin sections (Fig. 4A-B). *Leupoldina* is a genus of planktonic foraminifera, with numerous occurrences in the Tethyan region[54], that is used in global foraminiferal biozonation schemes[55]. Among the *Leupoldina* species (*L. cabri, L. pustulans, L. pentacamerata, L. hexacamerata*, and *L. reicheli*), *L. reicheli* rarely presents bifurcation in the last chamber, which is otherwise very characteristic for the other four species, particularly *L. cabri*[54]. Most of the specimens found in borehole 1PS-06-CE (39,20 m) show clear last chamber bifurcation (Fig. 4A), which leads us to exclude *L. reicheli* as a species candidate for those bifurcate specimens.

This consideration is important, as *L. reicheli*˜ s stratigraphic range is the widest among *Leupoldina* species (from *Leupoldina cabri* to *Globigerinelloides algerianus* zones[55], while the other four species range from biozones *L. cabri* to *Globigerinelloides ferreolensis*[55]. We assigned the corresponding interval to biozones *L. cabri* to *G. ferreolensis*[55], which corresponds to the early Aptian/early late Aptian stage[1] (Fig. 5). This outcome challenges the local biostratigraphic framework[27,56] and implies that the previous understanding of the chronostratigraphic framework for this post-rift sequence in the Araripe Basin must be reviewed.

Concerning the local zonation schemes, the presence of the age-indicative ostracods *Pattersoncypris* spp. and *Theriosynoecum silvai* at boreholes 1PS-06-CE and 1PS-10-CE suggests the local Alagoas Stage (Aptian–early Albian) for both sites (Zone 011, *sensu* Moura[58,59]; also called the *Pattersoncypris* and *Krommelbeincypris* Zone[60].

Furthermore, the occurrence of age-indicative pollen grains belonging to the species *Inaperturopollenites turbatus* (local Zone P-260[61]) constrains the studied intervals to an early late Aptian age. The uppermost occurrence of this taxon, however, does not represent its last occurrence datum, since a previous study found a continuous record of the same index species through most of the overlying Romualdo Formation[30]. Moreover, the absence of marker palynomorphs from older biozones (*I. curvimuratus* and *Tucanopollis crisopolensis*) also support an age as young as late Aptian[61].

The lack of representatives of typical lower Aptian palynomorph-based biozones is probably due to paleoclimate exclusion. Recent reconstructions of atmospheric circulation patterns suggest that a proto-Intertropical Convergence Zone (proto-ITCZ) played a key role in paleoflora distribution in Northeastern Brazil during the Early Cretaceous[62]. We contend that paleoclimate dynamics might have controlled the local appearance and disappearance of plant species, which directly affected the palynostratigraphic records.

Multi-proxy evidence of marine incursions

Three marine transgressive events, here named Araripe Marine Incursions (AMI), are clearly identifiable in the Barbalha Formation (Fig. 6). The Depositional Sequence 1 (*sensu* Assine et al.[14]) starts with very coarse- to coarse-grained sandstone facies (St2), superimposed by layers of fine- to very fine-grained sandstone with ripples (Sr3) (Fig. 7; Table 1). Muddy levels (F6 and F1) are observed in lateral associations, sometimes interbedded with rippled sandstone (Sr3), and as suggested previously, correspond to fluvial braided channels with laterally well-developed overbank[63] (Fig. 7; Table 1).

Paleocurrent data reveal preferential flow towards SE[14,22,40,63]. The presence of agglutinating foraminifera in sandstone deposits (1PS-10-CE) suggests brackish conditions[64] and might indicate deltaic influence in this fluvial system.

The fluvial braided channels and overbank deposits are overlaid by fine-grained facies of the Batateira Beds[65]. The facies observed in the Batateira Beds are siliciclastic (F1 and F2), intercalated with heterolithic facies (Hsr). They have been classified as a lacustrine system (Fig. 7; Table 1), due to the occurrence of non-marine elements such as ostracods, fish, and continental palynomorphs (e.g.,[23,66–68]). We have also verified the abundance of non-marine ostracod fauna (*Pattersoncypris micropapillosa*, *P. salitrensis*, *P. angulata*, *Pattersoncypris* sp. 1, *Pattersoncypris* sp. 2, *Candonopsis alagoensis*, and *Candona*? Sp.) in the deposits studied (Fig. 3A-H). Otherwise, ichnological and micropaleontological data support the input of marine waters in two distinct intervals, producing a salinity gradient between brackish to freshwater conditions in a lacustrine paleoenvironment.

The first marine incursion (AMI-1) is observed in both boreholes, just above the transgressive surface TS-1 (Fig. 7). It is marked by the presence of abundant agglutinated foraminifera and the occurrence of calcareous and organic-walled dinocysts. These marine elements occur in association with ichnofabric composed of *Planolites*, *Palaeophycus*, and *Thalassinoides* with low ichnodiversity, localized and restricted to facies F1, which points to the establishment of opportunistic colonization due to the onset of brackish conditions[69–71].

The second marine incursion, AMI-2, is observed in the middle part of the Batateira Beds associated with the laminite deposits of the C facies and corresponds to the maximum flooding surface (MFS-1). It is inferred based on the recovery of local marine elements such as calcareous and organic-walled dinocysts[72], calcareous nannofossils (*Thoracosphaera* spp. and ascidian spicules), serpulid tubes, and agglutinated foraminifera (*Bathysiphon* 1PS-10-CE). The thickness of these lacustrine deposits increases towards SE (borehole 1PS-06-CE: approximately 30 m thick) (Fig. 7). The presence of marine elements just above the TS-1 and in the middle of these lacustrine deposits (MFS-1), resting above the fluvial facies of both wells, reveals that there was a generalized flooding event associated with an increase in the relative sea level.

During the AMI-2 event, non-marine ostracod carapaces are particularly abundant in borehole 1PS-06-CE (more than 1,000 specimens recovered at the depths of 99.80 and 99.30 m), and the assemblage contains a large amount of well-preserved juvenile instars and adults, all with closed carapaces, indicating that they died at that life stage (Fig. 4G-J). Unusually, carapaces of adult *Pattersoncypris*, a mixohaline genus, are smaller than usual[60]. All these features are likely the result of development under a stressful environment and, eventually, a mass mortality event (e.g.,[73,74]). This could have been caused by salinity changes in the depositional setting of the Batateira Beds, as these ostracods did not tolerate fully marine conditions. This mortality event, associated with the presence of serpulids (Fig. 4I-J), foraminifera, calcareous nannofossils, and dinoflagellate cysts, reinforces the hypothesis of the establishment of full marine conditions during this interval. Towards the top, the Batateiras Bed record reestablishment of lacustrine environments following sea-level drop.

The overlying coarse-grained facies record subaerial exposure and the reactivation of the fluvial system and the beginning of Depositional Sequence 2, as interpreted by Assine et al.[14] and Scherer et al.[63]. The fluvial system strongly eroded the lake system deposits, creating a clear sequence boundary (SB) (Fig. 7). Paleocurrent measurements taken from outcrops (e.g., Rio Batateira) show predominant paleoflow towards a SE direction[14,22,40,63,68] Sandy deposits (Gt, Sgt, St1, and St2) related to fluvial channels are predominant in proximal settings (borehole 1PS-10-CE), and facies F2 and F3 represent overbank deposits in an underdeveloped floodplain within the river system[40,52,63]. The blocky and slickensides structures, associated with rhizobioturbation in F3 facies, also indicate eventual subaerial exposure[75].

Down depositional dip and above the SB in the borehole 1PS-06-CE, bioturbation is characterized by ichnofabric composed of *Planolites*, *Palaeophycus*, *Thalassinoides*, and *Cylindrichnus*, as well as monospecific ichnofabrics *Thalassinoides* (Hsr, F1, and F3). This set of ichnofabrics with low ichnodiversity and low bioturbation scale (BS = 1–2) reflects stressful conditions[69–71] and are related to the colonization of softgrounds, possibly stressed by salinity fluctuations (e.g.,[76]). They are an expression of the impoverished ichnofacies of *Cruziana* due to the appearance of brackish conditions in the distal part of the fluvial setting.

Ichnodiversity increases towards the top in distal settings, where bioturbation (Srd, Srw, St4) is represented by ichnofabric composed of *Diplocraterion*, *Ophiomorpha*, *Palaeophycus*, *Planolites*, *Thalassinoides*, *Chondrites*, *Helmintopsis*, *Scolicia*, *Lockeia*, and *Skolithos*. A moderate to high bioturbation index (BS 4–5) (Fig. 2) indicates the establishment of an impoverished expression of the mixed *Skolithos-Cruziana* ichnofacies (e.g.,[76,77]), and marks the beginning of AMI3. These ichnological characteristics might reflect stressful conditions caused by salinity changes. Moreover, the presence of *Scolicia* associated with the Srw lithofacies suggests that salinity was sufficient to sporadically support the establishment of a stenohaline fauna.

Scolicia has been mainly recorded in marine environments from shoreface to deep-sea (e.g.,[69,78–80]), and represents bioturbation by spatangoids echinoderms, which are truly marine organisms (e.g.,[81]). The

record of *Scolicia* in stressed substrates of distal, brackish, tidally dominated or influenced channels is scarce (e.g.,[82]). In addition, the higher ichnodiversity (ichnological assemblages) suggests increased marine conditions towards the top (Fig. 5).

The fluvial facies are overlain by muddy deposits (F3, F2, and F1) interbedded with sandstones (Sr, Srd, St2, and Sm). They are related to bayhead delta deposits[52] (Fig. 7; Table 1), suggesting the flooding of the fluvial system. The ichnological assemblages and micropaleontological data support this interpretation of flooding in both boreholes.

In borehole 1PS-10-CE, the bioturbation above the TS-2 is characterized by an ichnofabric composed of *Diplocraterion*, *Thalassinoides*, *Palaeophycus*, *Planolites*, *Chondrites*, *Cylindrichnus*, *Helminthopsis*, *Scolicia*, *Teichichnus*, and *Skolithos*, with BS 3–4. They are restricted to the Srd, and St2 lithofacies (Fig. 7). This ichnological assemblage is indistinguishable from the one observed in the fluvial deposits of the SE portion (1PS-06-CE), and points towards the establishment of an impoverished expression of the mixed *Skolithos-Cruziana* ichnofacies (e.g.,[76,77]) and continuous marine influence in the deposits.

The higher ichnodiversity, including *Scolicia* burrows (1PS-06-CE borehole), suggests marine conditions were more stable in the SE area. In addition, organic-walled-dinocysts are observed associated to this ichnofauna in facies F2 and F3 of both boreholes, reinforcing the input of marine waters in the depositional system. Finally, the occurrence of planktonic foraminifera (*Leupoldina* and globigerinelloids) in 1PS-06-CE, laterally associated with ichnological assemblages of the impoverished mixed *Skolithos-Cruziana* ichnofacies of 1PS-10-CE, suggests that marine to brackish conditions followed the onset of the bayhead delta. However, the presence of *Leupoldina* and globigerinelloids point to the establishment of typical marine conditions in the upper Barbalha Formation corresponding to the second maximum flooding surface (MFS-2) (Fig. 7).

Conclusions

We date the deposits of the Barbalha Formation for the first time based on recovery of the planktonic foraminifera genera *Leupoldina*. The morphology observed excludes the possibility of the *Leupoldina* spp. recovered being *L. reicheli*, meaning that the interval falls into the *L. cabri* to *G. ferreolensis* zones, which corresponds to the early Aptian/early late Aptian interval.

Three marine incursions (AMI-1 to AMI-3) were identified in the Barbalha Formation based on a multi-proxy analysis (micropaleontological, ichnological, and sedimentary analyses), with two of them occurring in the Batateira Beds. They record the primeval marine incursions in Araripe Basin related to the breakup of the Gondwana and the opening of the South Atlantic Ocean.

AMI-1, near the base of the Batateira Beds (lower Barbalha Formation), is characterized by an abundance of the agglutinated foraminifera *Bathysiphon* sp., and the minor occurrence of organic-walled dinocysts (*Exochosphaeridium majus*, *Oligosphaeridium poculum*, and some undetermined peridinioids) and calcareous dinocysts (*Thoracosphaera* spp.).

AMI-2 is characterized by organic-walled (abundant endocysts *Subtilisphaera* spp.) and calcareous dinocysts (*Thoracosphaera* spp.), ascidian spicules, microbial peloids, and abundant serpulid tubes in the laminite deposits of the Batateira Beds. The mass mortality event of non-marine ostracods reinforces this marine incursion event.

AMI-3 is characterized by the occurrence of a bioturbation ichnofabric composed of *Scolicia*, *Diplocraterion*, *Thalassinoides*, *Ophiomorpha*, *Teichichnus*, *Lockeia*, *Rizocorrallium*, and *Chondrites*. In addition, planktonic foraminifera association of *Leupoldina* spp. and *Globigerinelloides* spp. in the upper part of the Barbalha Formation indicates biozones *L. cabri/ G. ferreolensis*.

These incursions are the oldest recorded to date related to the breakup of the Gondwana and the opening of the South Atlantic Ocean. Future studies with fossils, geochemistry, and paleomagnetism will contribute to the characterization of these marine deposits, as well as the routes taken by these marine incursions.

Materials And Methods

Sedimentary Sections

We described and analyzed cores from boreholes 1PS-06-CE and 1PS-10-CE drilled by the Santana II Project[83] in the eastern portion of the Araripe Basin, Northeastern Brazil. Lithological, ichnological, microbiofaciological, and micropaleontological analyses were developed using samples from these boreholes. Sampling was preferentially done in the fine siliciclastic and limestone lithologies (shales, mudstones, siltstones, marls, and laminites), in addition to some sandstone levels. For further details, we provide the full dataset of microfossils/microbiofacies in the supplementary materials (SM).

Sedimentological, ichnological, and stratigraphic analysis

The sedimentary facies characterization of the 1PS-06-CE and 1PS-10-CE boreholes followed the usual methods, with the description of physical sedimentary structures and basic lithology, focusing on lithofacies and ichnology. The facies code utilized was adapted from Miall[84]. Intervals with no recovery were interpreted based on the accompanying well drilling data, namely gamma-ray values (indirect data); a small portion was obtained from cutting samples. For the purposes of stratigraphic correlation, the laminite deposits of the Batateira Beds, in the lower part of the Barbalha Formation, were chosen as our datum.

Direct macroscopic observation was used to describe trace fossils, following the main ichnotaxobases applicable to ichnofabrics: burrow limit, burrow infill, branching pattern, and presence/absence of spreiten. The guidelines used for ichnotaxonomy classification followed Bertling et al.[85]. In some cases, identification of ichnotaxa was hampered by the loss of the ichnotaxonomical features of the trace fossils present, dark lithology, and/or core deformation, which erased this data, as well as the restrictions inherent to observations made using two-dimensional core surfaces.

The amount of bioturbation was quantified considering the average diameter of 4 cm for the cores and using the bioturbation scale (BS) proposed by Reineck[86], which ranges from 0 (non-bioturbated) to 6 (completely bioturbated). Data from the Batateira River outcrop[14,51] was taken into consideration for the creation of the stratigraphic section, due to its geographical proximity and relevant correlation to the stratigraphic sequence.

Calcareous microfossils

Samples were prepared for the recovery of both ostracods and foraminifera using the methodology developed for the rocks of the Romualdo Formation used by Bom et al.[74], and consisted of the immersion of 20 g of sediment in 200 mL of deionized water with 3 mL of Extran for 24 hours. The sediments were then washed through 250, 180, 63, and 45 µm sieves, and dried for 48 in a lab oven at 40 ºC. After picking, we imaged the most representative specimens in an EVO/MA15 Zeiss scanning electron microscope (SEM).

Taxonomic suprageneric classification of ostracods followed Horne et al.[87] and Brandão et al.[88]. The classification of agglutinated foraminifers was based on Kaminsky[89]. All the studied material is currently stored in the micropaleontologic collection of Museu de História Geológica do Rio Grande do Sul (MHGRS), Unisinos University, Brazil, under the curatorial numbers ULVG 13571 to ULVG 13670.

Organic-walled microfossils

We processed approximately 40 g of each sediment sample for palynology analysis, following standard techniques[90]. Minimums of 300 and 500 palynomorphs were counted in each sample for the palynological and palynofacies methods, respectively. Species scanning, identification and counting were carried out with a Zeiss Imager.A2 microscope, using bright field illumination and incident blue light (fluorescence mode) at 200×, 400×, and 1000× (oil) magnifications. Photomicrographs were taken using a Zeiss AxioCam MRc (Micropaleontology Reference Center) digital camera. Our palynological analysis recorded pollen grains, spores, dinoflagellate cysts, and fresh water green algae, in addition to the phytoclasts and amorphous organic matter (AOM) recorded by palynofacies analysis. The slides are stored in the collection of the MHGRS, Unisinos University, Brazil, under the curatorial numbers ULVG 13482 to ULVG 13570.

Calcareous nannofossils

Sample preparation for calcareous nannofossil analysis followed the decantation methodology described in Bown and Young[91]. Each sediment sample was fragmented in an agate mortar and placed in a Falcon tube with 40 mL of deionized water. The solution was stirred for 30 seconds and then set to decant for five minutes. The supernatant (approximately 0.2 mL) was then collected, poured onto a coverslip, and placed in a hotplate (60°C) to dry. After dried, the coverslip was placed on a slide with Norland optical adhesive 61 and cured under UV light.

The slides were examined using a Zeiss Axio Imager.A2 microscope, at 1000× magnification. Data was processed using the software Zen 3.0 (blue edition) for micrometric measurements. The slides are stored in the collection of the Museum of Geological MHGRS, Unisinos University, Brazil, under the curatorial numbers ULVG 13671 to ULVG 13726.

Microbiofacies

Lithology (from both calcareous and clastic rocks) and preservation degree throughout the cored sections controlled the sampling interval we utilized. Select intervals of alternated mudstone-packstone and shale-siltstone required higher sampling density, while coarser-grained intervals were strategically undersampled.

We used a ZEISS Axioscope 5 petrographic microscope for microfossil identification and lithologic analysis, with transmitted and polarized light, objectives of 2.5×, 5×, 10×, and 20× magnification, and an attached digital camera. Data was processed using the software Zen 3.0 (blue edition) for micrometric measurements.

Calcareous rocks were described according to the nomenclatures of Dunham[92] and Embry and Klovan[93]. The taxonomic classification of planktonic foraminifera used was based on Sliter[94], Verga and Premoli-Silva[54,57], as well as the online Mesozoic Planktonic Foraminifera database located at www.mikrotax.org (pforams@mikrotax[55]). Planktonic foraminifera zones were defined based on the biostratigraphic schemes of Ogg[1]. We defined six semi-quantitative categories representing relative abundance, based on the number of specimens of foraminifera counted: very abundant (> 40), abundant (20–40), common (10–20), few (5–10), rare (3–5), and very rare (1–3) (SM).

Declarations

Acknowledgments

The authors acknowledge the research and development project entitled “Mar Interior: Incursões marinhas e a bioestratigrafia do Cretáceo Inferior nas Bacias Interiores do Nordeste do Brasil,” sponsored by Petrobras S.A., for funding this study; the National Mining Agency (Agência Nacional de Mineração – ANM/Brazil) for providing the studied samples; and itt Oceaneon/Unisinos for providing the facilities during the preparation, processing, and analytical steps. We are also grateful to Alessandra da Silva dos Santos, Daniela Reháková, Gerson José Salamoni Terra, Guilherme Krahl, and Renata Guimarães Netto for their helpful taxonomic and paleoecological discussions; and to Victória Herder Sander, Bruna Poatskievick Pierezan, Geovani Goulart Freitas, Lucas Vinicius Oliveira, Luciana Rigon Carneiro Duarte, and Valeska Meirelles, for all laboratory support during sample preparation, and processing techniques. GF was sponsored by Conselho Nacional de Desenvolvimento Científico e Tecnológico (CNPq/Brazil: grant number 308087/2019-4), and MLA is a research fellow of CNPq (grant number 310955/2021-1).

Author responsibilities

G.F, F.H.O.L., M.L.A., and O.S.J. designed the project. H.P.K., A.S.C., and J.V.M. conducted the stratigraphical, sedimentological, and ichnological studies. M.A.L.M. and L.M.L. performed the descriptive research of palynomorphs. M.A.B.S.F. and D.C. performed the descriptive research of ostracods. F.L.S. and O.S.J. performed the descriptive research of microbiofacies and foraminifera. A.N.A., E.J.F.T., and M.D.R.B. performed the descriptive research of calcareous nannofossils. S.B.F. and M.H.H.B. gave a critical review to the work. All authors reviewed the manuscript.

Declaration of competing interest

The authors declare that they have no known competing financial interests or personal relationships that could have appeared to influence the work reported in this paper.

Data availability

The authors confirm that the data supporting the findings of this study are available within the article and its supplementary materials.

References

1. Ogg, J. G., Ogg, G. M. & Gradstein, F. M. Cretaceous. in *A Concise Geologic Time Scale* 167–186 (Elsevier, 2016). doi:10.1016/b978-0-444-59467-9.00013-3.
2. Leckie, R. M., Bralower, T. J. & Cashman, R. Oceanic anoxic events and plankton evolution: Biotic response to tectonic forcing during the mid-Cretaceous. Paleoceanography **17**, 13-1-13–29 (2002).
3. Hay, W. W. Evolving ideas about the Cretaceous climate and ocean circulation. Cretaceous Research **29**, 725–753 (2008).
4. Haq, B. U. Cretaceous eustasy revisited. Global and Planetary Change vol. 113 44–58 (2014).
5. Dummann, W. *et al.* The impact of Early Cretaceous gateway evolution on ocean circulation and organic carbon burial in the emerging South Atlantic and Southern Ocean basins. Earth and Planetary Science Letters **530**, (2020).
6. Poulsen, C. J., Barron, E. J., Arthur, M. A. & Peterson, W. H. Response of the mid-Cretaceous global oceanic circulation to tectonic and CO2 forcings. Paleoceanography **16**, 576–592 (2001).
7. Moulin, M., Aslanian, D. & Unternehr, P. A new starting point for the South and Equatorial Atlantic Ocean. Earth-Science Reviews **98**, 1–37 (2010).
8. Matos, R. M. D., Krueger, A., Norton, I. & Casey, K. The fundamental role of the Borborema and Benin–Nigeria provinces of NE Brazil and NW Africa during the development of the South Atlantic Cretaceous Rift system. Marine and Petroleum Geology **127**, 104872 (2021).

9. Channell, J. E. T., Erba, E., Nakanishi, M. & Tamaki, K. Late Jurassic-Early Cretaceous Time Scales and Oceanic Magnetic Anomaly Block Models. in *Geochronology, Time Scales and Global Stratigraphic Correlation* (SEPM Society for Sedimentary Geology, 1995). doi:10.2110/pec.95.04.0051.
10. Gee, J. S. & Kent, D. v. Source of Oceanic Magnetic Anomalies and the Geomagnetic Polarity Timescale. Treatise on Geophysics **5**, 455–507 (2007).
11. Malinverno, A., Hildebrandt, J., Tominaga, M. & Channell, J. E. T. M-sequence geomagnetic polarity time scale (MHTC12) that steadies global spreading rates and incorporates astrochronology constraints. Journal of Geophysical Research: Solid Earth **117**, 1–17 (2012).
12. Ogg, J. G., Hinnov, L. A. & Huang, C. Cretaceous. in *The Geologic Time Scale 2012* 793–853 (Elsevier B.V., 2012). doi:10.1016/B978-0-444-59425-9.00027-5.
13. Arai, M. Aptian/Albian (Early Cretaceous) paleogeography of the South Atlantic: a paleontological perspective. Brazilian Journal of Geology vol. 44 339–350 (2014).
14. Assine, M. L. *et al.* Sequências deposicionais do Andar Alagoas da Bacia do Araripe, Nordeste do Brasil. Boletim de Geociências da Petrobras **22**, 3–28 (2014).
15. Bobco, F. E. R., Goldberg, K. & Bardola, T. P. Modelo deposicional do Membro Ipubi (Bacia do Araripe, nordeste do Brasil) a partir da caracterização faciológica, petrográfica e isotópica dos evaporitos. Pesquisas em Geociências **44**, 431 (2017).
16. Goldberg, K., Premaor, E., Bardola, T. & Souza, P. A. Aptian marine ingression in the Araripe Basin: Implications for paleogeographic reconstruction and evaporite accumulation. Marine and Petroleum Geology **107**, 214–221 (2019).
17. Beurlen, V. K. Geologia e estratigrafia da Chapada do Araripe. in *XVII Congresso Brasileiro Geologia* (SBG/SUDENE, 1963).
18. Beurlen, V. K. Novos equinóides no Cretáceo do Nordeste do Brasil. Anais da Academia Brasileira de Ciências **389**, 455–464 (1966).
19. Beurlen, V. K. As condições ecológicas e faciológicas da Formação Santana na Chapada do Araripe (Nordeste do Brasil). Anais da Academia Brasileira de Ciências **43**, 411–415 (1971).
20. Braun, O. P. G. *Estratigrafia dos sedimentos da parte inferior da região nordeste do Brasil (bacias do Tucano-Jatobá, Mirandiba e Araripe)*. vol. 236 (Divisão de Geologia e Mineralogia/DNPM, 1966).
21. Mabesoone, J. M. & Tinoco, I. M. Palaeoecology of the Aptian Santana Formation (Northeastern Brazil). Palaeogeography, Palaeoclimatology, Palaeoecology **14**, 97–118 (1973).
22. Assine, M. L. Paleocorrentes e paleogeografia na Bacia do Araripe, Nordeste do Brasil. Revista Brasileira de Geociências **24**, 223–232 (1994).
23. Assine, M. L. Bacia do Araripe. Boletim de Geociências da Petrobras **15**, 371–389 (2007).
24. Ponte, F. C. & Appi, C. J. Proposta de revisão da coluna litoestratigráfica da Bacia do Araripe. in *36º Congresso Brasileiro de Geologia* vol. 36 211–226 (1990).

25. Brito Neves, B. B., Santos, E. J. & van Schmus, W. R. Tectonic history of the Borborema Province. in *Tectonic evolution of the South America. 31st International Geological Congress* (eds. Cordani, U. G., Milani, E. J., Thomaz Filho, A. & Campos, D. A.) 151–182 (IUGS, 2000).
26. Fambrini, G. L. *et al. Caracterização dos sistemas deposicionais da Formação Barbalha, Bacia do Araripe, nordeste do Brasil*. vol. 103 http://www.lneg.pt/iedt/unidades/16/paginas/26/30/209 (2016).
27. Coimbra, J. C., Arai, M. & Carreño, A. L. Biostratigraphy of Lower Cretaceous microfossils from the Araripe Basin, northeastern Brazil. Geobios **35**, 687–698 (2002).
28. Martill, D. M. The age of the Cretaceous Santana Formation fossil Konservat Lagerstätte of north-east Brazil: a historical review and an appraisal of the biochronostratigraphic utility of its palaeobiota. Cretaceous Research **28**, 895–920 (2007).
29. Tomé, M. E. T. R., Lima Filho, M. F. & Neumann, V. H. M. L. Taxonomic studies of non-marine ostracods in the Lower Cretaceous (Aptian-lower Albian) of post-rift sequence from Jatobá and Araripe basins (Northeast Brazil): Stratigraphic implications. Cretaceous Research vol. 48 153–176 (2014).
30. Arai, M. & Assine, M. L. Chronostratigraphic constraints and paleoenvironmental interpretation of the Romualdo Formation (Santana Group, Araripe Basin, Northeastern Brazil) based on palynology. Cretaceous Research **116**, 104610 (2020).
31. Melo, R. M. *et al.* New marine data and age accuracy of the Romualdo Formation, Araripe Basin, Brazil. Scientific Reports **10**, (2020).
32. Araripe, R. C. *et al.* Upper Aptian–lower Albian of the southern-central Araripe Basin, Brazil: Microbiostratigraphic and paleoecological inferences. Journal of South American Earth Sciences **116**, 103814 (2022).
33. Assine, M. L. Sedimentação e Tectônica da Bacia do Araripe, Nordeste do Brasil. 1–124 (1990).
34. Neumann, V. H. & Assine, M. L. Stratigraphic proposal to the post-rift I tectonic sedimentary sequence of Araripe Basin, Northeastern Brazil. in *2nd International Congress on Stratigraphy* (PAGES International Project, 2015).
35. Benigno, A. P. A., Saraiva, A. Á. F., Sial, A. N. & Lacerda, L. D. Mercury chemostratigraphy as a proxy of volcanic-driven environmental changes in the Aptian-Albian transition, Araripe Basin, northeastern Brazil. Journal of South American Earth Sciences **107**, 103020 (2021).
36. Lúcio, T., Souza Neto, J. A. & Selby, D. Late Barremian / Early Aptian Re–Os age of the Ipubi Formation black shales: Stratigraphic and paleoenvironmental implications for Araripe Basin, northeastern Brazil. Journal of South American Earth Sciences **102**, (2020).
37. Barreto, A. M. F. *et al.* U/Pb geochronology of fossil fish dentine from Romualdo Formation, Araripe Basin, northeast of Brazil. Journal of South American Earth Sciences **116**, 103774 (2022).
38. Assine, M. L. Análise estratigráfica da Bacia do Araripe, Nordeste do Brasil. Revista Brasileira de Geociências **22**, 289–300 (1992).

39. Chagas, D. B. Litoestratigrafia da Bacia do Araripe: reavaliação e propostas para revisão. *Dissertation (MSc)* 1–112 (2006).
40. Fambrini, G. L. *et al.* Análise tectonossedimentar das fases início de rifte e clímax de rifte da Bacia do Araripe, Nordeste do Brasil. Geologia USP. Série Científica **19**, 205–236 (2019).
41. Catto, B., Jahnert, R. J., Warren, L. V., Varejao, F. G. & Assine, M. L. The microbial nature of laminated limestones: Lessons from the Upper Aptian, Araripe Basin, Brazil. Sedimentary Geology **341**, 304–315 (2016).
42. Warren, L. V. *et al.* Stromatolites from the Aptian Crato Formation, a hypersaline lake system in the Araripe Basin, northeastern Brazil. Facies **63**, 1–19 (2017).
43. Varejão, F. G. *et al.* Exceptional preservation of soft tissues by microbial entombment: Insights into the taphonomy of the Crato Konservat-Lagerstätte. Palaios **34**, 331–348 (2019).
44. Custódio, M. A. *et al.* The transgressive-regressive cycle of the Romualdo Formation (Araripe Basin): Sedimentary archive of the Early Cretaceous marine ingression in the interior of Northeast Brazil. Sedimentary Geology **359**, 1–15 (2017).
45. Fürsich, F. T. *et al.* Analysis of a Cretaceous (late Aptian) high-stress ecosystem: The Romualdo Formation of the Araripe Basin, northeastern Brazil. Cretaceous Research **95**, 268–296 (2019).
46. Rodrigues, M. G. *et al.* Short-lived “Bakevelliid-Sea” in the Aptian Romualdo Formation, Araripe Basin, northeastern Brazil. Cretaceous Research **115**, (2020).
47. Silva-Santos, R. & Valença, J. G. A Formação Santana e sua paleoictiofauna. in Anais da Academia Brasileira de Ciências 339–358 (1968).
48. Maisey, J. G. *Santana Fossils: An Illustrated Atlas*. (T.H.F. Publications, 1991).
49. Arai, M., Neto, J. B., Lana, C. C. & Pedrao, E. Cretaceous dinoflagellate provincialism in Brazilian marginal basins. Cretaceous Research **21**, 351–366 (2000).
50. Teixeira, M. C., Mendonça Filho, J. G., Oliveira, A. D. de & Assine, M. L. Faciologia orgânica da Formação Romualdo (Grupo Santana, Cretáceo Inferior da Bacia do Araripe): caracterização da matéria orgânica sedimentar e interpretação paleoambiental. Geologia USP. Série Científica **17**, 19 (2016).
51. Araripe, R. C., Oliveira, D. H., Tomé, M. E., Moura de Mello, R. & Barreto, A. M. F. Foraminifera and Ostracoda from the Lower Cretaceous (Aptian–lower Albian) Romualdo Formation, Araripe Basin, northeast Brazil: Paleoenvironmental inferences. Cretaceous Research **122**, 104766 (2021).
52. Varejão, F. G. *et al.* Mixed siliciclastic–carbonate sedimentation in an evolving epicontinental sea: Aptian record of marginal marine settings in the interior basins of north-eastern Brazil. Sedimentology **68**, 2125–2164 (2021).
53. Luft-Souza, F. *et al.* Sergipe-Alagoas Basin, Northeast Brazil: A reference basin for studies on the early history of the South Atlantic Ocean. Earth-Science Reviews 104034 (2022) doi:10.1016/J.EARSCIREV.2022.104034.

54. Verga, D. & Premoli-Silva, I. Early Cretaceous planktonic foraminifera from the Tethys: the genus Leupoldina. Cretaceous Research **23**, 189–212 (2002).
55. Huber, B. T. *et al.* Pforams@microtax: A new online taxonomic database for planktonic foraminifera. Micropaleontology **62**, 429–438 (2016).
56. Rios-Netto, A. D. M., Regali, M. D. S. P., Carvalho, I. D. S. & Freitas, F. I. de. Palinoestratigrafia do intervalo Alagoas da Bacia do Araripe, Nordeste do Brasil. Revista Brasileira de Geociências **42**, 331–342 (2012).
57. Verga, D. & Premoli-Silva, I. Early Cretaceous planktonic foraminifera from the Tethys: the large, many-chambered representatives of the genus Globigerinelloides. Cretaceous Research **24**, 661–690 (2003).
58. Moura, J. A. Biocronoestratigrafia da seqüencia não marinha do Cretáceo Inferior da Bacia de Campos, Brasil: Ostracodes. in *10th Congresso Brasileiro de Paleontologia, Rio de Janeiro, Anais* vol. 2 717–731 (1987).
59. Moura, J. A. Ostracods from Non-marine Early Cretaceous sediments of the Campos Basin, Brazil. Developments in Palaeontology and Stratigraphy **11**, 1207–1216 (1988).
60. Poropat, S. F. & Colin, J.-P. Early Cretaceous ostracod biostratigraphy of eastern Brazil and western Africa: An overview. Gondwana Research **22**, 772–798 (2012).
61. Regali, M. S. P. & Silva Santos, P. R. Palinoestratigrafia e geocronologia dos sedimentos Albo-Aptianos de Sergipe-Alagoas. in *Boletim do 5° Simpósio sobre o Cretáceo do Brasil* 411–419 (UNESP - Campus de Rio Claro/SP, 1999).
62. Santos, A. *et al.* Earlier onset of the Early Cretaceous Equatorial humidity belt. Global and Planetary Change **208**, 103724 (2022).
63. Scherer, C. M. S., Goldberg, K. & Bardola, T. Facies architecture and sequence stratigraphy of an early post-rift fluvial succession, Aptian Barbalha Formation, Araripe Basin, northeastern Brazil. Sedimentary Geology **322**, 43–62 (2015).
64. Radley, J. D. A foraminiferal datum in the Vectis Formation (Wealden Group, Lower Cretaceous) of the Isle of Wight, southern England. *Proceedings of the Geologists' Association* **105**, 91–97 (1994).
65. Hashimoto, A. T., Appi, C. J., Soldan, A. L. & Cerqueira, J. R. O Neo-Alagoas nas bacias do Ceará, Araripe e Potiguar (Brasil): Caracterização estratigráfica e paleoambiental. Revista Brasileira de Geociências **17**, 118–122 (1987).
66. Lima, M. R. & Perinotto, J. A. J. Palinologia de sedimentos da parte superior da Formação Missão Velha, Bacia do Araripe. Geociências **3**, 67–76 (1984).
67. Neumann, V. H., Borrego, A. G., Cabrera, L. & Dino, R. Organic matter composition and distribution through the Aptian-Albian lacustrine sequences of the Araripe Basin, northeastern Brazil. International Journal of Coal Geology **54**, 21–40 (2003).
68. Chagas, D. B., Assine, M. L. & Freitas, F. I. Facies sedimentares e ambientes deposicionais da Formação Barbalha no Vale do Cariri, Bacia do Araripe, Nordeste do Brasil. Geociências UNESP **26**, 313–322 (2007).

69. Uchman, A. An opportunistic trace fossil assemblage from the flysch of the Inoceramian beds (Campanian-Palaeocene), Bystrica Zone of the Magura Nappe, Carpathians, Poland. Cretaceous Research **13**, 539–547 (1992).
70. Buatois, L. A., Saccavino, L. L. & Zavala, C. Ichnologic signatures of hyperpycnal flow deposits in Cretaceous river-dominated deltas, Austral Basin, southern Argentina. in (eds. Slatt, R. M. & Zavala, C.) 1–18 (AAPG Special Volumes, 2011). doi:10.1306/13271355St611948.
71. Buatois, L. A. & Mángano, M. G. *Ichnology: Organism-substrate interactions in space and time*. (Cambridge University Press, 2011).
72. Pons, D., Berthou, P.-Y. & Campos, D. A. Quelques observations sur la palynologie de l'Aptien Supérieur et de l'Albien du Bassin d'Araripe (NE du Brésil). in *Simpósio sobre a Bacia do Araripe e bacias interiores do Nordeste* 241–252 (DNPM/SBP/SBGeo, 1990).
73. Whatley, R. C. Population structure of ostracods: some general principles for the recognition of palaeoenvironments. in *Ostracoda in the earth sciences* (eds. DeDeckker, P., Colin, J. P., Peypouquet, J. P. & Townsend, A.) 231–244 (Elsevier Science Ltd, 1988).
74. Bom, M. H. H. *et al.* Paleoenvironmental evolution of the Aptian Romualdo Formation, Araripe Basin, Northeastern Brazil. Global and Planetary Change **203**, (2021).
75. Kraus, M. J. Paleosols in clastic sedimentary rocks: Their geologic applications. Earth Science Reviews **47**, 41–70 (1999).
76. Buatois, L. A. *et al.* Colonization of brackish-water systems through time: Evidence from the trace-fossil record. Palaios **20**, 321–347 (2005).
77. Pemberton, S. G. *et al.* Ichnology and Sedimentology of Shallow to Marginal Marine Systems: Ben Nevis & Avalon Reservoirs, Jeanne d'Arc Basin. *Geological Association of Canada Short Course Notes, St. John's* vol. 15 353 (2001).
78. Crimes, P. T. & Stuijvenberg, U. A. Trace fossil assemblages of deep-sea fan deposits, Gurnigel and Schlieren flysch (Cretaceous-Eocene), Switzerland. (1981).
79. Buatois, L. A., Bromley, R. G., Mángano, M. G., Bellosi, E. & Carmona, N. Ichnology of shallow marine deposits in the Miocene Chenque Formation of Patagonia: complex ecologic structure and niche partitioning in Neogene ecosystems. APA Publicación especial **9**, 85–95 (2003).
80. Carmona, N. B. *et al.* Scolicia and its producer in shallow-marine deposits of the Miocene Chenque Formation (Patagonia, Argentina): functional morphology and implications for understanding burrowing behavior. Ichnos: an International Journal of Plant and Animal **27**, 290–299 (2020).
81. Smith, A. B. & Crimes, P. T. Trace fossils formed by heart urchins - a study of Scolicia and related traces. Lethaia **16**, 79–92 (1983).
82. Díez-Canseco, D., Buatois, L. A., Mángano, M. G., Rodriguez, W. & Solorzano, E. The ichnology of the fluvial–tidal transition: Interplay of ecologic and evolutionary controls. in *Developments in Sedimentology* vol. 68 283–321 (Elsevier, 2015).
83. Scheid, C., Munis, M. B. & Paulino, J. *Projeto Santana – Relatório Final Etapa II*. (1978).

84. Miall, A. D. *The geology of fluvial deposits: sedimentary facies, basin analysis, and petroleum geology*. (Springer, 1966).
85. Bertling, M. *et al.* Names for trace fossils: A uniform approach. Lethaia **39**, 265–286 (2006).
86. Reineck, H. E. *Sedimentgefüge im Bereich der südliche Nordsee*. vol. 505 (Abhandlungen der Senckenbergischen Naturforschenden Gesellschaft, 1963).
87. Horne, D. J., Cohen, A. & Martens, K. Taxonomy, morphology and biology of Quaternary and living Ostracoda. Washington DC American Geophysical Union Geophysical Monograph Series **131**, 5–36 (2002).
88. Brandão, S. N., Angel, M. v., Karanovic, I., Perrier, V. & Meidla, T. World ostracoda database. *Updated at* http://www. marinespecies. org/*ostracoda* https://marinespecies.org/aphia.php?p¼taxdetailsandid¼1078 (2019).
89. Kaminski, M. A. The year 2010 classification of the agglutinated foraminifera. Micropaleontology **60**, 239–255 (2004).
90. Wood, G. D. Palynological techniques-processing and microscopy. in *Palynology: Principles and Application* (eds. Jasonius, J. & McGregor, D. C.) vol. 1 29–50 (American association of stratigraphic palynologists foundation, 1996).
91. Bown, P. & Young, J. R. *Calcareous nannofossil biostratigraphy*. (Chapman and Hall; Kluwer Academic, 1998).
92. Dunham, R. J. Classification of carbonate rocks according to depositional textures. (1962).
93. Embry, A. F. & Klovan, E. J. A late Devonian reef tract on northeastern Banks Island, NWT. Bulletin of Canadian Petroleum Geology **19**, 730–781 (1971).
94. Sliter, W. v. Cretaceous planktic foraminiferal biostratigraphy of the Calera Limestone, northern California, USA. Journal of Foraminiferal Research **29**, 318–339 (1999).

Figures

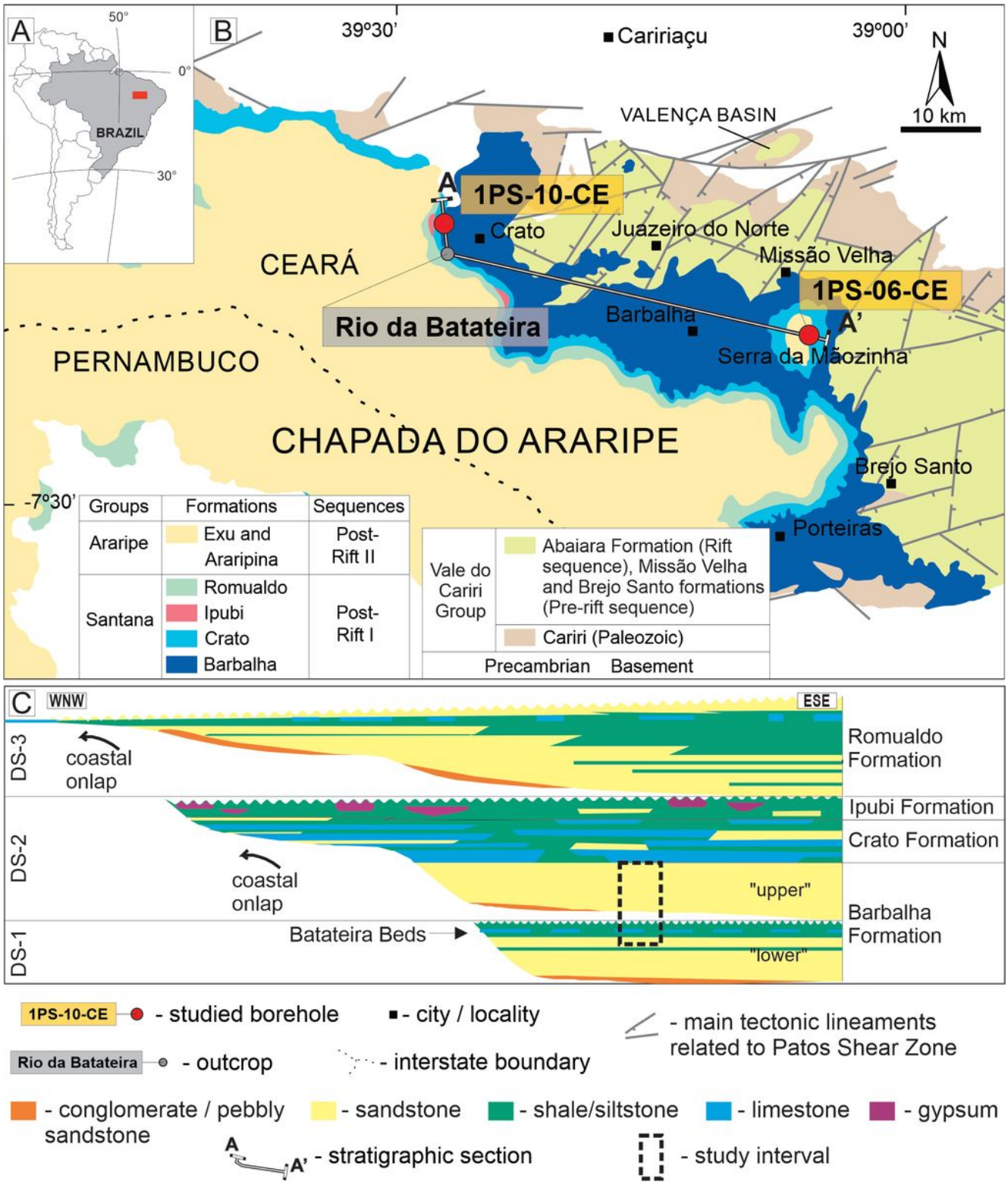

Figure 1

Geographic location and stratigraphic position of the studied area. A) Map of South America and studied area (red frame). B) Simplified geological map of the Araripe Basin with the location of the boreholes used in this study (modified from Assine et al.,[14]). C) Stratigraphic framework of the Alagoas Post-rift Stage in the Araripe Basin composed of three depositional sequences bounded by disconformities. SD-1

= depositional sequence 1; SD-2 = depositional sequence 2; and SD-3 = depositional sequence 3 (modified from Assine et al.,[14]).

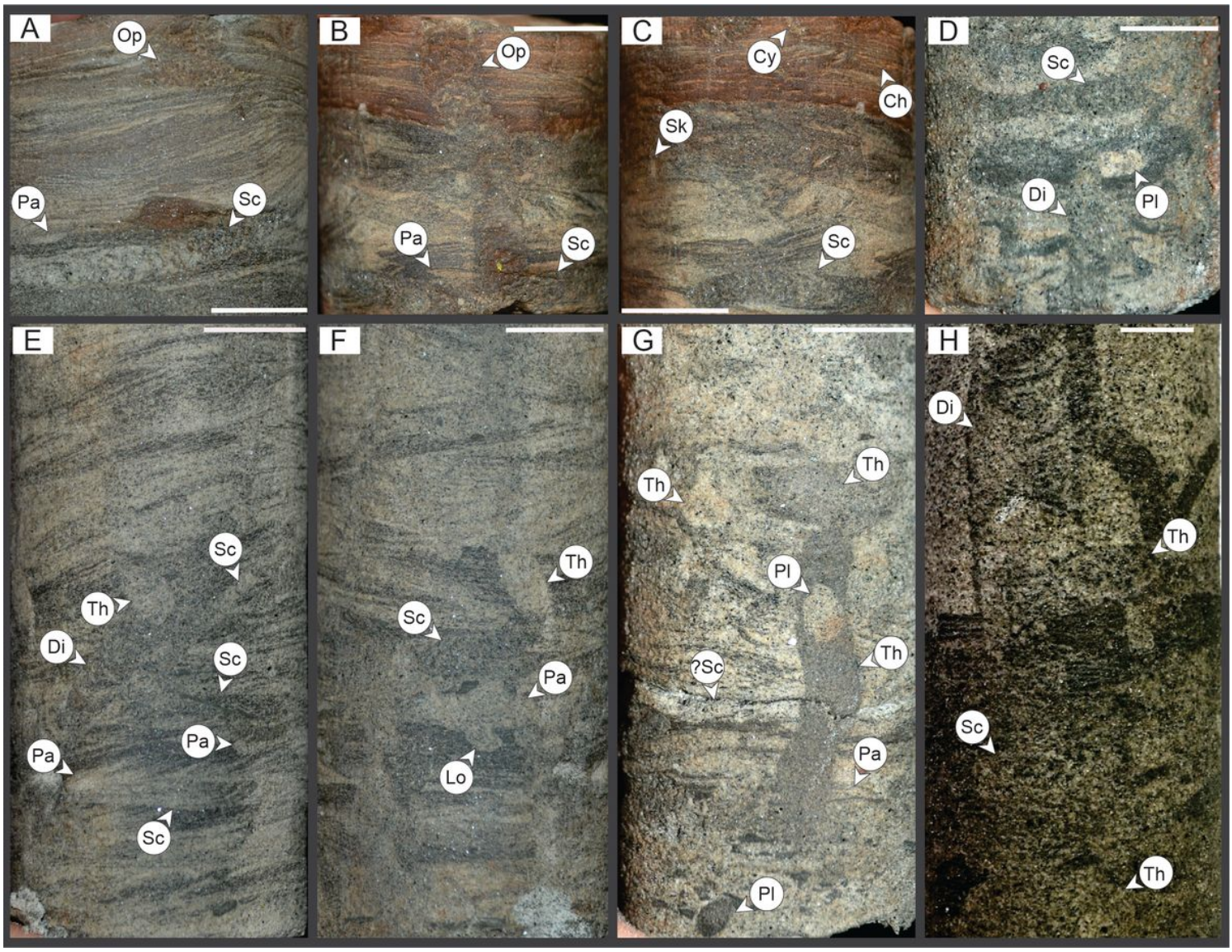

Figure 2

Traces fossils produced in softground substrate identified in the ichnofabrics of the studied section (Barbalha Formation) (1PS-06-CE and 1PS-10-CE boreholes). A-C) *Ophiomorpha* (Op), *Scolicia* (Sc), *Palaeophycus* isp (Pa), *Cylindrichnus* (Cy), *Skolithos* (Sk) (1PS-06-CE / 66.40 m). D) *Scolicia* (Sc), *Diplocraterium* (Di), *Planolites* (PL) (1PS-06-CE / 57.00 m). E-F) *Scolicia* (Sc), *Thalassinoides* (Th), *Diplocraterium* (Di), *Palaeophycus* (Pa), *Lockeia* (Lo) (1PS-06-CE / 68.50 m). G) *Thalassinoides* (Th), *Scolicia* (Sc), *Planolites* (Pl), *Palaeophycus* (Pa) (1PS-06-CE / 54.50 m). H) *Diplocraterium* (Di), *Thalassinoides* (Th), *Scolicia* (Sc) (1PS-10-CE / 33.50 m). Scale: 10 mm.

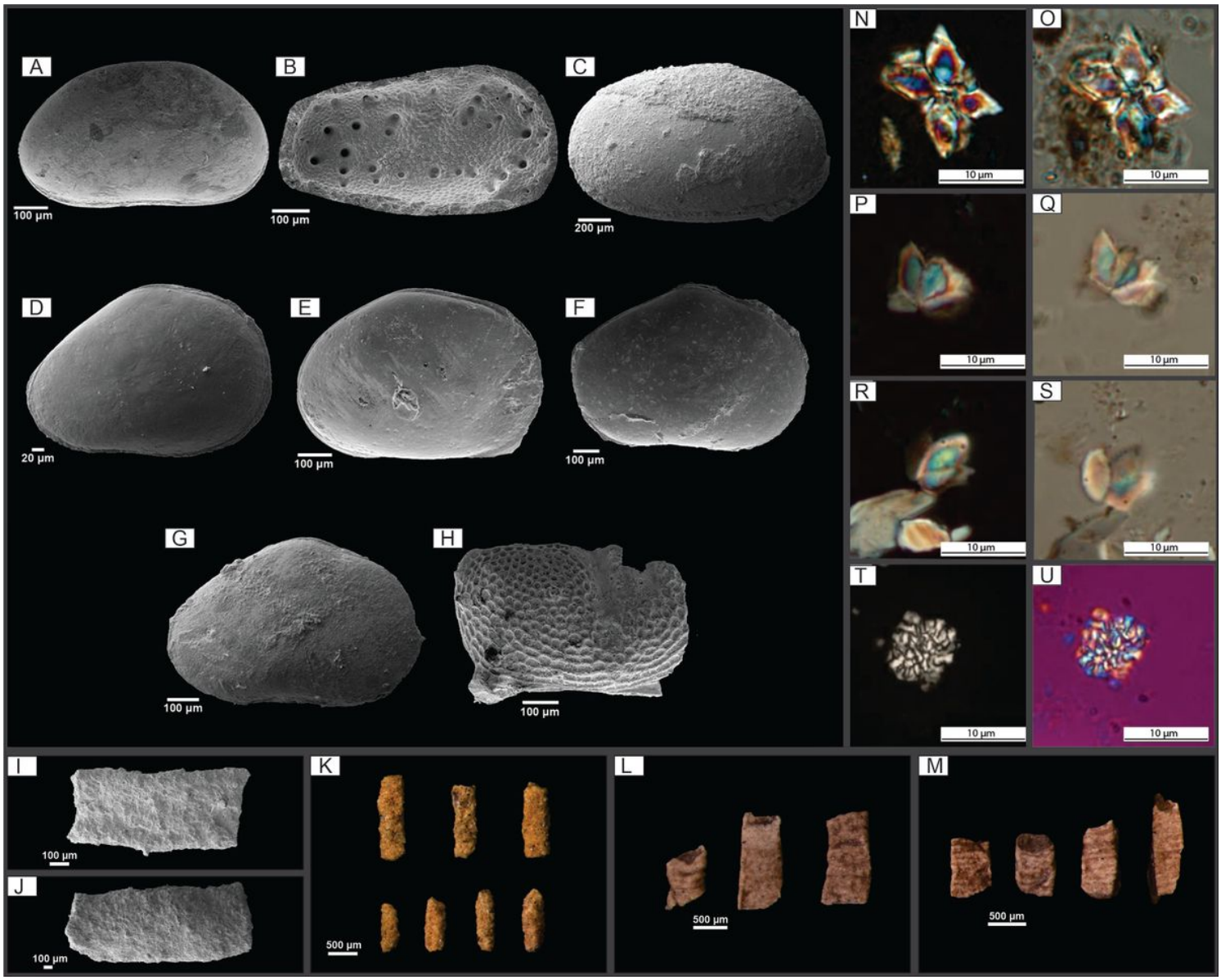

Figure 3

Plate illustrating key microfossil species recovered from boreholes 1PS-06-CE and 1PS-10-CE. Ostracods: A) *Candonopsis alagoensis* (right lateral view; 1PS-06-CE); B) *Cypridea* sp. (mold; 1PS-10-CE); C) *Brasacypris subovatum* (right lateral view; 1PS-10-CE); D) *Pattersoncypris alta*? (right lateral view; 1PS-06-CE); E) *Pattersoncypris salitrensis* (right lateral view; 1PS-06-CE); F) *Pattersoncypris angulata sensu* Tomé et al. (2014) (1PS-06-CE); G) *Pattersoncypris micropappilosa* (right lateral view; 1PS-06-CE); H) *Theriosynoecum silvai* (right valve; 1PS-06-CE). Foraminifers: I-M) *Bathysiphon* sp. (I-J: 1PS-06-CE, 117.90 m; K-M: 1PS-10-CE, 103.20 m, and 102.90 m). Calcareous nannofossils: N-S) Ascidian spicule (1PS-06-CE; 99.30 m). T-U) and *Thoracosphaera* spp. (1PS-06-CE; 114.70m).

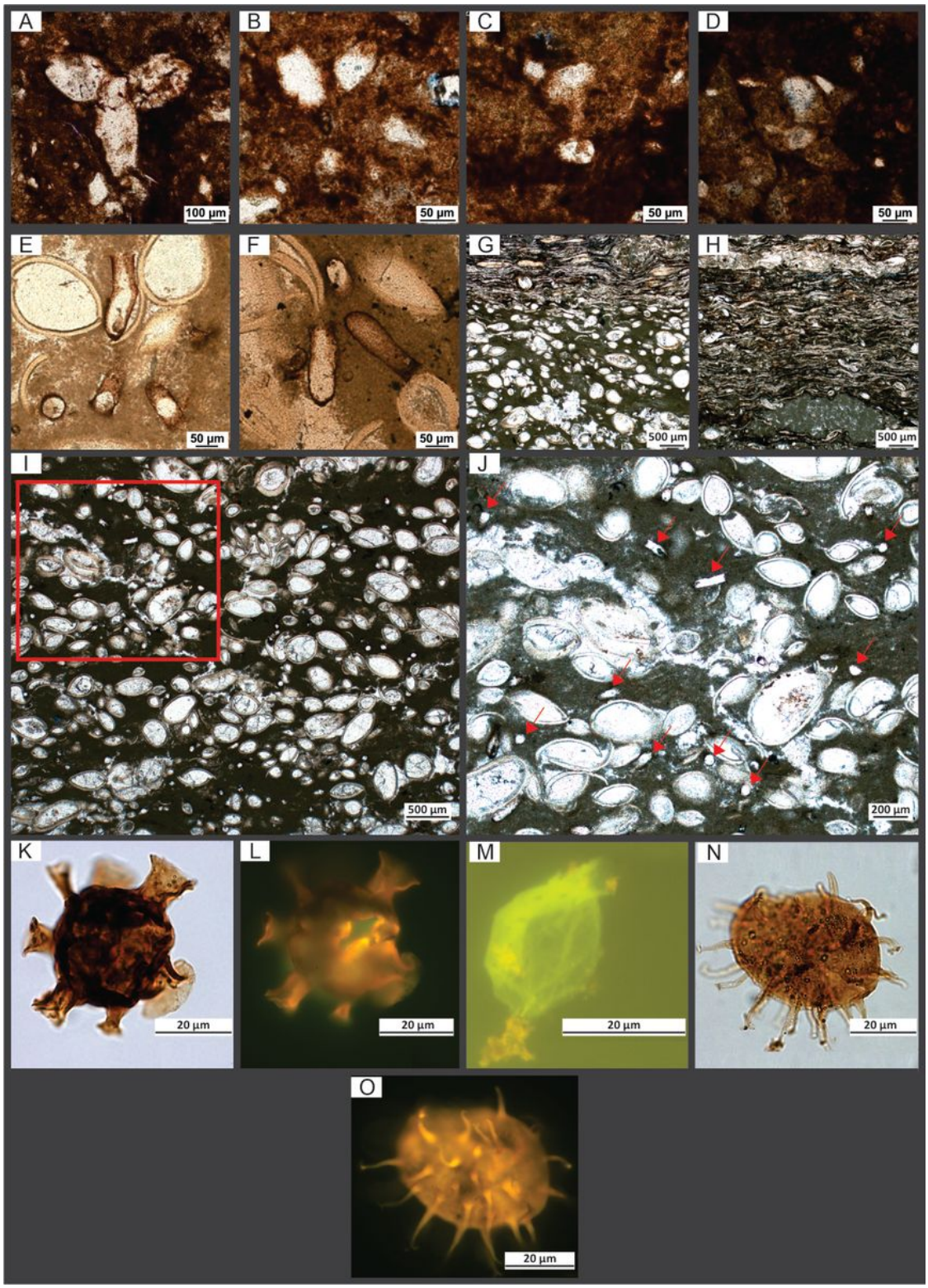

Figure 4

Plate illustrating key microfossil species recovered (1PS-06-CE and 1PS-10-CE boreholes). A-B) *Leupoldina* sp.; C) *Globigerinelloides* cf. *barri*; D) *Globigerinelloides* cf. *ferreolensis* (1PS-06-CE, 35 39,20m); E-F) Serpulids; G) Wackestone and packstone with ostracods; H) Packstone with ostracods; I) Wackestone with ostracods and serpulids (red frame corresponds to image “J”); J) Detail view of wackestone with ostracod shells and serpulid tubes (red arrows) (1PS-06-CE, 99,30m); K)

Oligosphaeridium poculum (1PS-06-CE, 115.8m; 100x4.5); L) *Oligosphaeridium poculum* (1PS-06-CE, 115.8m; 100x4.5; fluorescence mode); M) *Subtilisphaera* sp. (1PS-06-CE, 99.30m; 105.1x24.8; fluorescence mode); N) *Exochosphaeridium* majus (1PS-06-CE, 115.8m; 103.5x2.5); and O) *Oligosphaeridium poculum* (1PS-06-CE, 115.8m; 100x4.5; fluorescence mode).

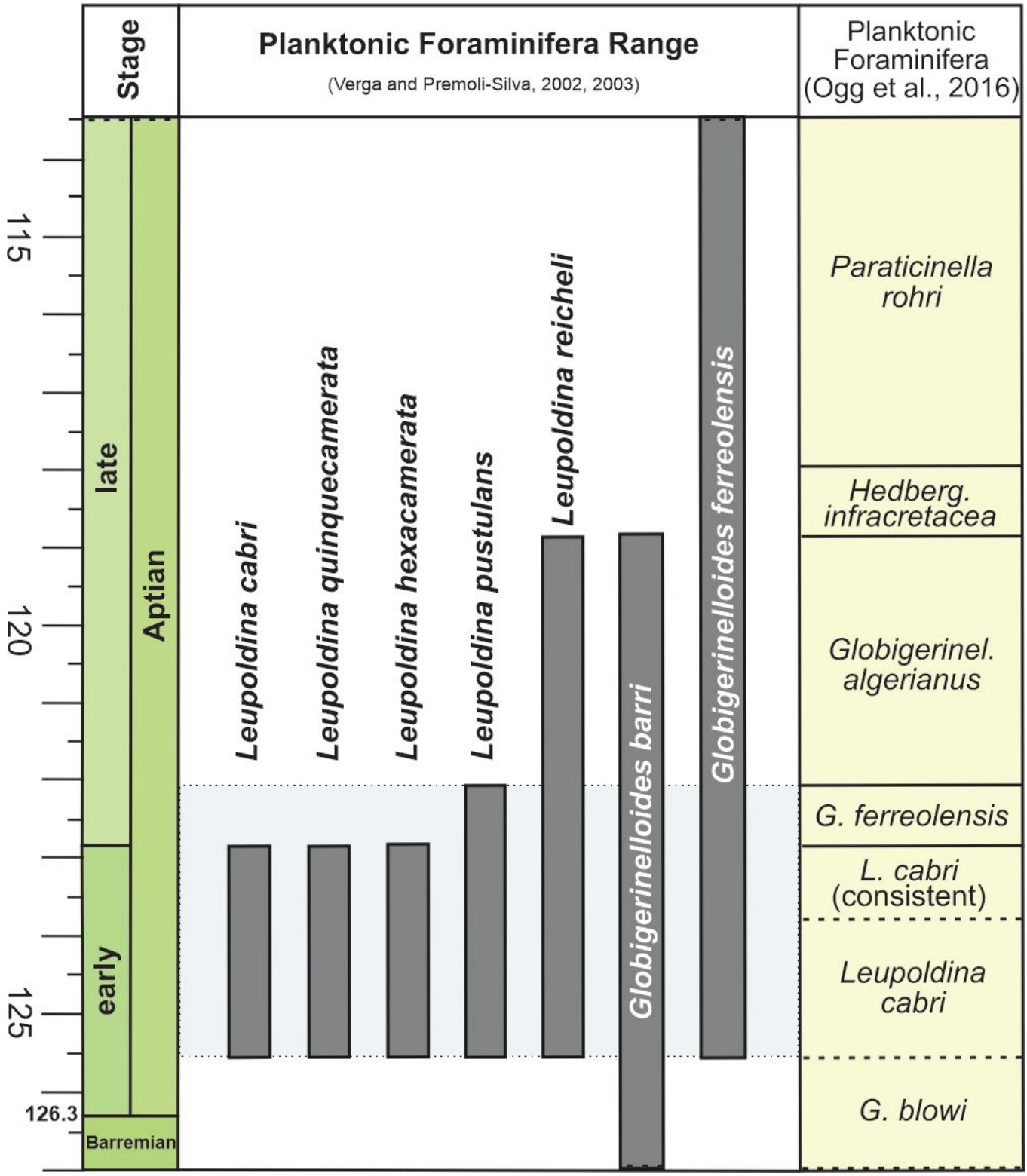

Figure 5

Planktonic foraminifera zonation scheme for the late Barremian–Aptian interval. Planktonic foraminifera range is taken from Verga and Premoli-Silva[54,57] (adapted of Ogg et al.[1]).

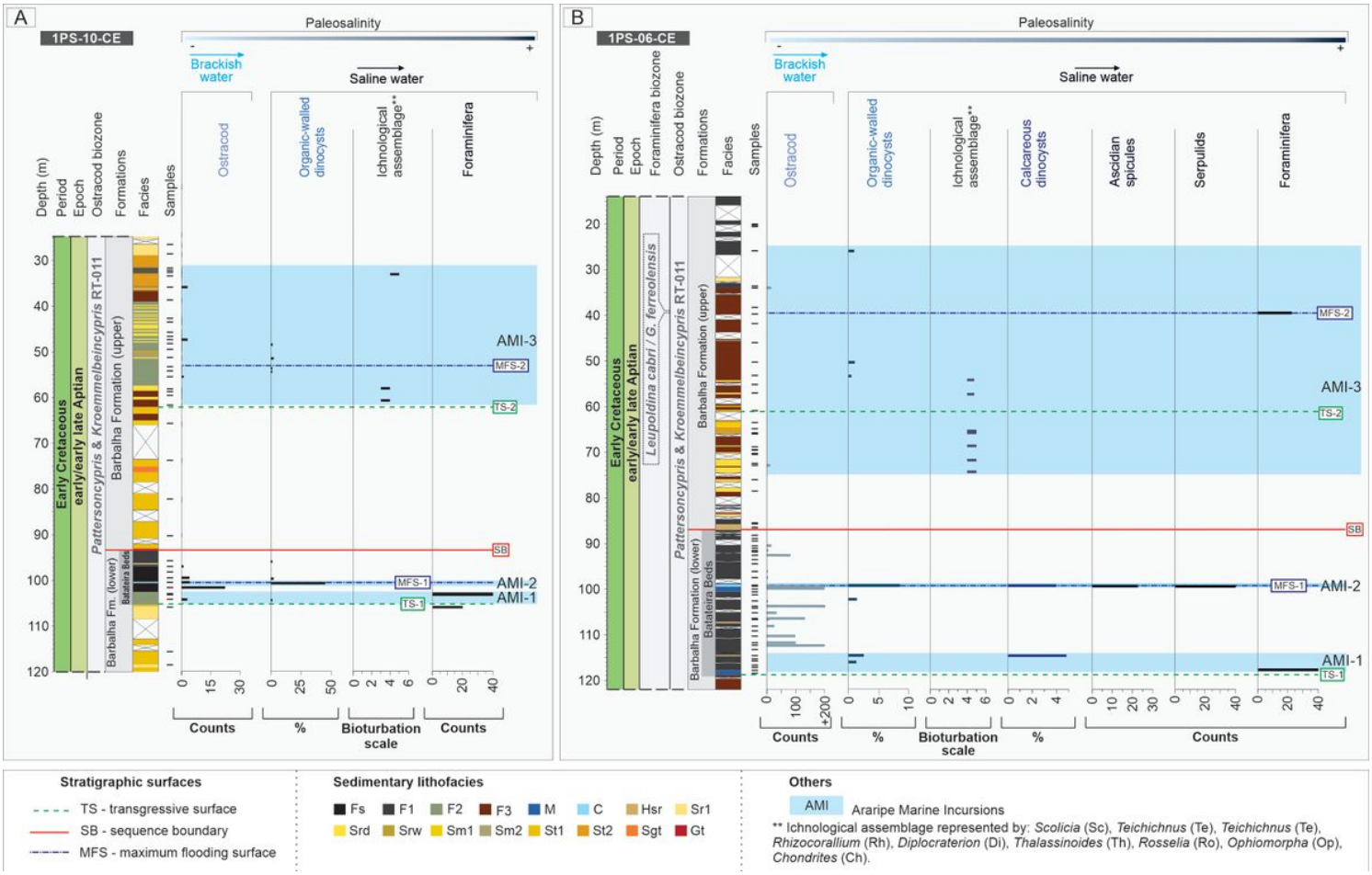

Figure 6

Composed plots of marine proxies' analyses. A) Paleosalinity indicator and demarcation of marine incursions in 1PS-10-CE borehole. B) Paleosalinity indicator and demarcation of marine incursions in 1PS-06-CE borehole.

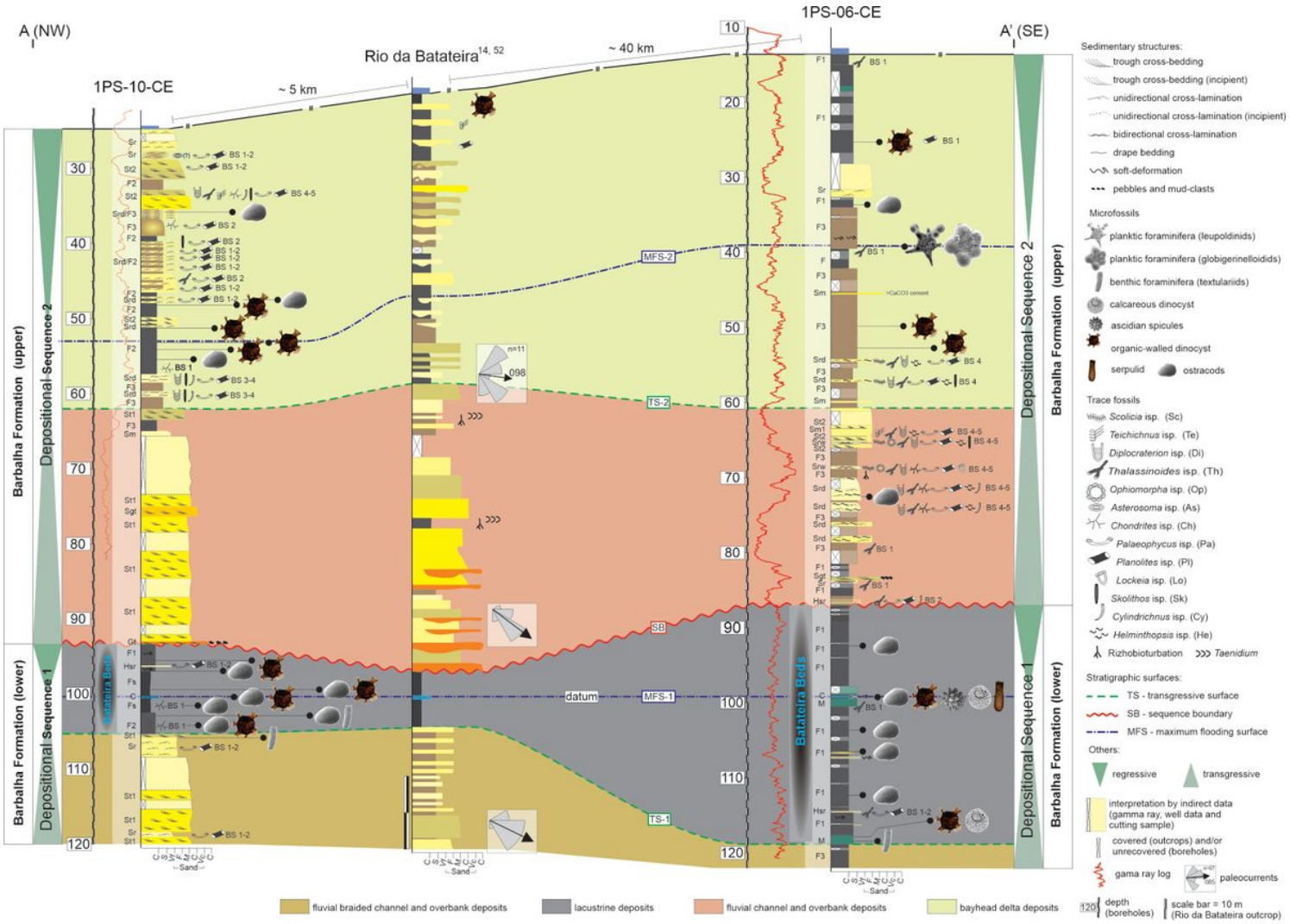

Figure 7

NW-SE stratigraphic section (location in Fig. 1B).

Supplementary Files

This is a list of supplementary files associated with this preprint. Click to download.

- SupplementaryMaterials.xlsx